Synthesis and characterization of mononuclear complexes of metals transition of 1,3-bis-((5-methyl-1*H*-imidazol-4-yl) methyleneamino) propan-2-ol

ABSTRACT

The ligand 1,3-bis-((5-methyl-1*H*-imidazol-4-yl)methyleneamino)propan-2-ol (H_3L) derived from 1,3-diaminopropan-2-ol and 5-methyl-1*H*-imidazole-4-carbaldehyde has been synthetized and used to prepare five complexes in which the ligand acts in tetradentate fashion. Complexes formulated as $[Mn(H_3L)(H_2O)_2]\cdot 2SCN$ (**1**), $[(Co(H_3L)]\cdot 2SCN$ (**2**), $[(Ni(H_3L)]\cdot 2SCN$ (**3**), $[(Cu(H_3L)(NO_3)]\cdot(NO_3)\cdot 2H_2O$ (**4**), and $[(Zn(H_3L)]\cdot 2SCN$ (**5**) were synthesized by mixing an equimolar amount of an methanol solution containing the appropriate nitrate salt and KSCN, in 1:2 ratio, in the case of **1**, **2**, **3** and **5** and an ethanol solution containing the appropriate ligand H_3L. The complex **4** has been synthetized in the absence of KSCN. In all the complexes the ligand acts in its neutral form and in tetradentate fashion, its hydroxy group remaining free and non-deprotonated. The ligand is coordinated to metal ion through two azomethine nitrogen atoms and two pyrazole sp^2 nitrogen atoms. The complexes are characterized by elemental analysis, conductance and room temperature magnetic moments measurements, UV–Vis and IR spectroscopic studies. The structure of the copper(II) complex **4** is confirmed by X-ray diffraction. **4** crystallizes in the monoclinic space group $P2_1/c$ with unit cell dimensions a = 8.5459 (3) Å, b = 10.9177 (3) Å, c = 22.4562 (6) Å, β = 96.954 (3)°, V = 2079.79 (11) Å^3, Z = 4, R_1 = 0.050 and wR_2 = 0.131. The Cu^{II} cation in N_4O inner is situated in a distorted square pyramidal environment.

Keywords: Crystal structure; manganese; cobalt; nickel; copper; zinc; square pyramidal.

1. INTRODUCTION

For a long time, chemists have used many metal ions to synthetize molecules with original properties [1, 2]. These metal ions that also participate in biological processes continue to attract increasing interest. Some metal complexes are used as anticancer [3], antifungal [4], antimicrobial [5], antituberculosis drugs [6], as magnetic materials [7] or as materials for optics [8]. Currently, transition metal (II) complexes are the subject of extensive research for a variety of functionalities and applications, such as medicine [9, 10] or catalysis [11, 12]. Schiff bases, which are molecules with several donor sites that can be soft or hard, occupy a central role in the coordination chemistry of metals. These Schiff bases have made it possible to prepare a large number of complexes with original structures and fabulous properties. They have made it possible to develop mimetic chemistry to study the complexes that intervene in biological processes [13–15]. Transition metal(II) complexes derived from symmetric or asymmetric Schiff bases have attracted considerable attention in the field of coordination chemistry due to their facile synthesis processes, fascinating structures, and wide ranges of diverse applications covering photochemistry [16], catalysis [17], and biomimicking [18]. In this regard, we synthesized a symmetric and flexible ligand with two arms that have coordination sites capable of encapsulating a metal ion. This ligand 1,3-bis-((5-methyl-1*H*-imidazol-4-yl)methyleneamino)propan-2-ol H_3L allowed the preparation of metal transition complexes (Mn, Co, Ni, Cu and Zn) which are characterized by spectroscopic studies and the structure of the copper(II) complex was solved by X-ray diffraction analysis.

2. MATERIAL AND METHODS

2.1. Starting materials and Instrumentations

1,3-diaminopropan-2-ol, 5-methyl-1*H*-imidazole-4-carbaldehyde, manganese nitrate tetrahydrate, cobalt nitrate hexahydrate, nickel nitrate hexahydrate, copper nitrate trihydrate and zinc nitrate

hexahydrate were commercial products (from Aldrich) and were used without further purifications. The solvents were reagent grade and were purified by usual methods. Elemental analyses were carried out using a VxRio EL Instrument. The FTIR spectra were recorded on a FTIR Spectrum Two of Perkin Elmer (4000–400 cm^{-1}). The UV–Visible spectra were run on a Perkin-Elmer UV/Visible spectrophotometer Lambda 365 (1000–200 nm). The ^{1}H and ^{13}C NMR spectra of the Schiff base were recorded in $CDCl_3$ on a BRUKER 500 MHz spectrometer at room temperature using TMS as an internal reference. The molar conductance of 10^{-3} M solutions of the metal complexes in DMF were measured at 25 °C using a WTW LF-330 conductivity meter with a WTW conductivity cell. Magnetic measurements for complexes were performed at room temperature by using a Johnson Mattey scientific magnetic susceptibility balance (Calibrant: $Hg[Co(SCN)_4]$).

2.2. Synthesis of the ligand 1,3-bis-((5-methyl-1*H*-imidazol-4-yl)methyleneamino)propan-2-ol (H_3L)

1,3-diaminopropan-2-ol (0.7119 g, 7.9 mmol) was introduced into a round bottomed flask containing 5 mL of methanol. 5-methyl-1*H*-imidazole-4-carbaldehyde (1.7397 g, 15.8 mmol) previously dissolved in 5 mL of methanol was added. The resulting yellow solution was refluxed for 4 hours. After cooling, the yellow precipitate formed was recovered by filtration. The solid was washed with 2x10 mL of ether then dry in a desiccator under P_2O_5. **FTIR (**v, cm^{-1}) : 3300 (**OH**), 1644 (C**=N)**$_{imine}$,1601(C=N) $_{imidazole,}$ 1580 ; 1437 (C_{Ar}=C_{Ar}). **RMN ^{1}H** ($CDCl_3$, 400MHz, δ(ppm)) : 8.10 (s, 2H, **H**C=N), 7.18 (s, 2H, **H**-imd), 6.43 (s, 2H, **H**N-imd), 6.19 (s, 1H, -O**H**), 4.15 (quint, 1H, -C**H**OH-) ; 3.55 (d, 4H, -(C**H**$_2$)$_2$) ; 2.26 (s, 6H, -(C**H**$_3$)).
RMN ^{13}C ($CDCl_3$, 400MHz, δ(ppm)) : 159.56 (H**C**=N), 140.58(H**C**=N$_{imid}$) 129.60 (Me-**C**=C-), 124.43 (Me-C=**C**-), 77.66 (-**C**H$_2$-), 71.11(-**C**H(OH)-), 15.07 (-CH_3).

2.3. Synthesis of the complexes of H_3L

H_3L (0.3 g; 1 mmol) was dissolved in a round bottomed flask containing 5 mL of methanol. The filtrate of the mixture containing $M(NO_3)_2{\cdot}nH_2O$ (M= Mn^{2+} (**1**), Co^{2+}(**2**), Ni^{2+}(**3**), Zn^{2+} (**5**)) (1 mmol) and KSCN (1 mmol) was added. The mixture was refluxed for 2 hours and then the clear solution obtained is filtered and left to evaporate slowly. Complex **4** is synthesized in absence of KSCN. After three weeks, the copper complex (**4**) gives blue single crystals suitable for X-ray diffraction analysis while the other complexes give powders characterizable by other techniques.

Table 1. Analytical data, room temperature magnetic moments and conductance of complexes 1-5.

Complexes	Yield (%)	Color	% C Calc. (Found)	% H Calc. (Found)	% N Calc. (Found)	Λ ($\Omega^{-1}{\cdot}cm^2{\cdot}mol^{-1}$)	μ_{eff} (μ_B)
H_3L	83	Yellow	56.92 (56.89)	6.61 (6.58)	30.64 (30.60)	-	-
$[Mn(H_3L)(H_2O)_2]{\cdot}2SCN$ (**1**)	32	Brown	37.42 (37.40)	4.61 (4.56)	23.27 (23.24)	140	5.61
$[(Co(H_3L)]{\cdot}2SCN$ (**2**)	31	Green	40.09 (40.06)	4.04 (4.00)	24.93 (24.90)	142	4.52
$[(Ni(H_3L)]{\cdot}2SCN$ (**3**)	42	Brown	40.11 (40.07)	4.04 (4.01)	24.95 (24.91)	138	Diam.

[(Cu(H_3L)(NO_3)]·(NO_3)·2H_2O (**4**)	67	blue	31.36 (31.33)	4.45 (4.41)	22.50 (22.46)	70	1.67
[(Zn(H_3L)]·2SCN (**5**)	63	Yellow	39.52 (39.48)	3.98 (3.95)	24.58 (24.56)	142	diam

2.4. X-ray structure determination of complex 4

Methanol solution of **4** was left to slow evaporation and yellow crystals suitable for X-ray analyze were formed after three weeks. The details of the X-ray crystal structure solution and refinement are given in Table 3. Measurements were made on a Bruker SMART CCD Area Detector. All data were corrected for Lorentz and polarization effects. Empirical absorption correction was applied. Complex scattering factors were taken from the program package *SHELXTL* [19]. The structures were solved by direct methods, which revealed the position of all non-hydrogen atoms. All the structures were refined on F^2 by a full-matrix least-squares procedure using anisotropic displacement parameters for all nonhydrogen atoms [20]. All hydrogen atoms were located in their calculated positions and refined using a riding model. Molecular graphics were generated using *ORTEP-3* [21].

3. RESULTS AND DISCUSSIONS

General study

The reaction of 1,3-bis-((5-methyl-1*H*-imidazol-4-yl)methyleneamino)propan-2-ol (H_3L) with $Mn(NO_3)_2{\cdot}4H_2O$, $Co(NO_3)_2{\cdot}6H_2O$, $Ni(NO_3)_2{\cdot}6H_2O$ or $Zn(NO_3)_2{\cdot}6H_2O$ in presence of KSCN or $Cu(NO_3)_2{\cdot}3H_2O$ in ethanol afforded mononuclear complexes. The reactions of the ligand with metal transition salts are depicted in scheme 1. Yields and analytical data are recorded in Table 1. The IR spectrum of the ligand H_3L shows two bands in the high frequency region located at 3300 cm^{-1} and 3114 cm^{-1} attributed, respectively, to the vibration valence $\nu_{O—H}$ of the alcohol function and the $\nu_{N—H}$ of the imidazole moiety (Table 2). The bands located at 1641 cm^{-1} and 1601 cm^{-1} are, respectively, due to the vibration bands $\nu_{C=N}$ of the azomethine moiety and the imidazole derivative [22]. The bands observed at 1580 cm^{-1} and 1437 cm^{-1} are attributed to the vibrations $\nu_{C=C}$ of the imidazole ring. The ^1H NMR spectrum of the proton of the ligand H_3L is recorded in $CDCl_3$. It shows a signal at 8.10 ppm characteristic of the protons of the azomethine functions. The signals pointed at 7.18 ppm and 6.43 ppm correspond, respectively, to the protons of -CH and -NH of the imidazole ring. The signal at 6.19 ppm is attributed to the proton of the -O—H function of the secondary alcohol. The signals observed in the form of a quintuplet at 4.15 ppm and the signal at 3.55 ppm in the form of a doublet are attributed, respectively, to the methylene protons and to the proton of the carbon bearing the OH group. The signal at 2.26 ppm corresponds to the two methyl groups of the imidazole ring. The J-modulated spectrum of the H_3L ligand recorded in chloroform allows the assignment of the ^{13}C signals. The signals of the quaternary carbon atoms of the imidazole ring are pointed at 129.60 and 124.42 ppm and that of the carbon bearing two protons is plotted at 77.66 ppm. These signals are oriented in one direction while the signals of the carbon atoms bearing an odd number of protons are oriented in the other direction. The azomethine carbon atoms give a signal at 159.56 ppm and the signal of the carbon atom of imidazole bearing a single proton is plotted at 140.58 ppm. The signals at 71.11 ppm and 15.07 ppm are attributed, respectively, to the carbon atom bearing the alcohol function and to the carbon atom of the methyl group. The strong and broad band due to $\nu_{O—H}$ and $\nu_{N—H}$ stretching are pointed in the regions [3324 cm^{-1} - 3419 cm^{-1}] and [3108 cm^{-1} - 3118 cm^{-1}] on the spectra of the complexes showing that the ligand interacts with the metal ions in its neutral form and that in some complexes there is presence of water molecule (Table 2). The bands pointed respectively at 1641 cm^{-1} and 1601 cm^{-1} on the spectrum of the free ligand are observed, respectively, in the range [1607 cm^{-1}- 1643 cm^{-1}] and [1589 cm^{-1} – 1604 cm^{-1}] on the spectra of the complexes. The shifts of these bands indicate the involvement of the nitrogen atoms of azomethine and imidazole nitrogen atoms in the coordination. A strong and sharp band pointed, respectively, at 2067 cm^{-1}, 2082 cm^{-1}, 2095 cm^{-1} and 2073 cm^{-1} on the spectra of

manganese (**1**), cobalt (**2**), nickel (**3**) and zinc (**5**) complexes are attributed to the $\nu_{S=C=N}$ vibration band of the free thiocyanate [23]. The spectrum of the complex $[Cu(H_3L)(NO_3)]\cdot(NO_3)\cdot 2(H_2O)$ (**4**) presents bands suggesting the presence of a free nitrate and a coordinated nitrate groups. Indeed, the strong and sharp band present at 1366 cm^{-1} [24] indicates the presence of a free NO_3^- ion. The bands at 1323 cm^{-1}, 1258 cm^{-1}, 1180 cm^{-1} are due, respectively, to the ν_1, ν_2 and ν_5 vibrations of the coordinated nitrate group. The coordination mode is discussed by the parameter $\Delta\nu = \nu_1 - \nu_5$ [24]. The value of $\Delta\nu$ which is 143 cm^{-1} indicates the monodentate character of the coordinated nitrate group.

Table 1 : Main IR and electronic bands of the ligand H_3L and its complexes.

	$\nu_{O—H}$	$\nu_{N—H}$	$\nu_{C=N}$	$\nu_{C=Nimid}$	$\nu_{C=C}$	ν_{3NO_3}	ν_{1NO_3}	ν_{2NO_3}	ν_{5NO_3}	λ (nm)
H_3L	3300	3114	1641	1601	1580	-	-	-	-	272, 289, 296
(**1**)	3421	3118	1635	1592	2067	-	-	-	-	271, 288, 296, 322, 440, 539
(**2**)	3324	3108	1607	1595	2082	-	-	-	-	271, 288, 296, 402, 442, 532
(**3**)	3326	3109	1634	1589	2095	-	-	-	-	271, 288, 296, 435
(**4**)	3419	3109	1643	1604		1366	1363	1258	1180	242, 271, 295, 460, 605
(**5**)	3327	3111	1621	1590	2073	-	-	-	-	271, 288, 296,

Conductance

Conductimetric measurements of millimolar solutions of all complexes were recorded in dimethylformamide (DMF) solution (Table 1). Two series of measurements at fifteen-day intervals were carried out to find the nature of the electrolyte and monitor the stability of the complexes in solution. The molar conductivity value of the freshly prepared solution of the copper complex $[Cu(H_3L)(NO_3)]\cdot(NO_3)\cdot 2(H_2O)$ (**4**) which is 70 $Ohm^{-1}\cdot cm^2\cdot mol^{-1}$ is in agreement with the value reported for 1:1 electrolyte type [25]. The molar conductivity values of the complexes **1**, **2**, **3** and **5** are in the range [138 – 142] $Ohm^{-1}\cdot cm^2\cdot mol^{-1}$. These values are characteristic of 1:2 electrolyte type [25]. After fifteen days, the molar conductivity values of all the complexes remain constant, suggesting that the complexes are stable in solution in DMF.

Electronic spectra and magnetism

The room temperature magnetic moments of the paramagnetic complexes are recorded in Table 1. The electronic spectra data of H_3L and the complexes **1**-**5** are shown in Table 2. The spectrum of the ligand H_3L exhibits three bands at 272 nm, 289 nm, and 296 nm which were assigned to $\pi\rightarrow\pi^*$ and $n\rightarrow\pi^*$ transitions. The Mn(II) complex (**1**) exhibits two additional bands at 440 nm and 539 nm which are assigned to the $^6A_{1g}\rightarrow{}^4T_{1g}$ and $^6A_{1g}\rightarrow{}^4T_{2g}$ transitions, respectively, corresponding to octahedral geometry for a Mn(II) ion [26]. The magnetic moment value of 5.61 μ_B for the complex **1** at room temperature is compatible with the value of 5.92 μB expected for a Mn(II) ion in high spin state with a d^5 configuration. This value fall in the range [5.2 μ_B – 6.0 μ_B] for Mn(II) complex in octahedral geometry [27]**.** The electronic spectrum of the cobalt(II) (**2**) complex present three bands at 402, 442 and 532 nm, which clearly indicate the low-spin square planar geometry of the complex [28]. The observed effective magnetic moment of the complex (**2**) [2.65 μ_B] corresponds to one unpaired electron d^7 cobalt ion in square planar the geometry [29]. The electronic spectrum of the nickel(II) (**3**) shows an additional single band pointed at 435 nm assignable to $^1A_{1g}\rightarrow{}^1B_{1g}$, which is consistent with a square planar geometry around Ni(II) ion [30]. The magnetic moment measurement shows that the complex is diamagnetic confirming the square planar geometry [31]. The electronic spectrum of the complex of Cu(II) (**4**) shows two bands with low intensities at 605 and 460 nm which are assigned to $^2B_{1g}\rightarrow{}^2A_{1g}$ and $^2B_{1g}\rightarrow{}^2E_g$ transitions, respectively. The $^2B_{1g}\rightarrow{}^2B_{2g}$ transition is not observed owing to the low intensities in the spectrum [32]. These observation are consistence with a square pyramidal geometry around the Cu(II) ion [33]. The value of the room temperature magnetic moment value of 1.67 μ_B is consistence with square pyramidal geometry around the Cu(II) ion. The d^{10} configuration zinc complex is diamagnetic. The environment of the tetracoordinated Zn(II) can be described as a square planar geometry or as a tetrahedral geometry.

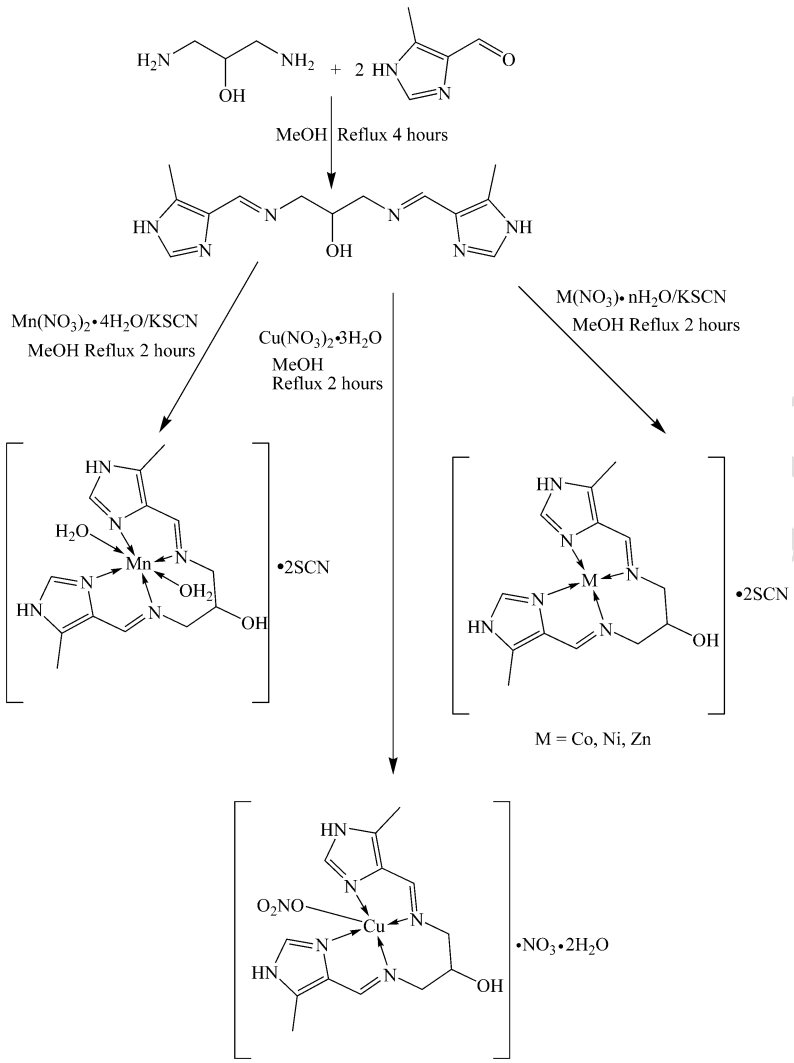

Scheme 1. Synthetic procedure of the ligand H_3L and its metal transition complexes.

Description of the structure of 4

The complex crystallizes in the monoclinic system with the space group $P2_1/c$. The selected interatomic distances and angles are given in the Table 4. The asymmetric unit contains one neutral ligand molecule, one Cu(II) ion, one coordinated nitrate group, one uncoordinated nitrate group, and two uncoordinated water molecules. The ligand acts in tetradentate fashion through two azomethine nitrogen atoms and two pyrazole nitrogen atoms, while the hydroxyl group remains free. One of the nitrate groups is monodentate through an oxygen atom. The copper atom is pentacoordinated and is located in an N_4O site. After coordination, the ligand forms two five-membered rings of type CuNCCN with bit angle values of 82.67 (9)° and 82.40 (9)°.The environment of a pentacoordinated metal ion can be described using the Addison parameter $\tau = (\beta - \alpha)/60$ (β and α are the largest values of the bond angles around the central atom) [34] : $\tau = 0$ describes a perfect square pyramidal while $\tau = 1$ describes a perfect trigonal–bipyramidal geometry. The τ value of 0.0358 is indicative of a slightly distorted square pyramidal geometry around Cu1. The basal plane is occupied by N2, N3, N4 and N5, the apical position being occupied by the nitrate O3 atom. The Cu(II) ion is situated 0.074 Å out of the mean plane defined by the atoms occupying the basal plane. The *cissoid* bond-angle values [82.40 (9)° – 101.74 (9)°] as well as the *transoid* bond-angle values [174.46 (9)° and 173.10 (8)°] deviate severely from the ideal value of 90° and 180°, respectively, for a perfect square pyramidal geometry. Additionally, the bond-angle values between the atom occupying the apical position and the atoms in the basal plane [88.80 (12)° - 96.78 (12)°] deviate considerably from the ideal value of 90°. The sum of the angles subtended by the atoms in the basal plane, which is equal to 359.69°, deviates

slightly from the ideal value of 360°. The Cu—N_{imine} [Cu1—N3 = 1.995 (2) Å and Cu1—N4 = 2.002 (2) Å] are comparable to the Cu—$N_{imidazol}$ [Cu1—N2 = 1.996 (2) Å and Cu1—N5 = 1.993 (2) Å] (Table 1). The Cu—O3 bond distance [2.424 (4) Å] is the longest distance owing to the Jahn-teller effect [35]. These distances are in accordance with the results reported for similar complexes [36].

Table 3. Crystallographic data and refinement parameters for complex 4.

Chemical Formula	$[Cu(H_3L)(NO_3)]\cdot(NO_3)\cdot 2(H_2O)$
*M*r	497.92
Crystal shape/color	Cut block/blue
Crystal system, space group	Monoclinique, $P2_1/c$
Crystal size (mm)	0.10 × 0.10 × 0.05
a (Å)	8.5459 (3)
b (Å)	10.9177 (3)
c (Å)	22.4562 (6)
β (°)	96.954 (3)
V (Å^3)	2079.79 (11)
Z	4
D_{calc} (g.cm^{-3})	1.590
λ (MoKα) (Å)	0.71073
T (K)	293
μ (mm^{-1})	1.11
Index ranges	-11 ≤ *h* ≤ 11, -14≤ *k*≤ 13, -30≤ *l*≤ 27
F(000)	1028
θ range (°)	3.656-29.361
No. of measured reflections	22594
No. of independent reflections	4980
No. of observed [*I*> 2σ(*I*)] reflections	4044
R_{int}	0.043
$R[F^2 > 2\sigma(F^2)]$	0.050
w$R(F^2)$	0.134
Goodness-of-fitt (Gof) on F^2	1.09
No. of parameters	382
No. of restraints	92
$\Delta\rho_{max}$, $\Delta\rho_{min}$ (e Å^{-3})	1.08, − 0.45

Table 4. Selected geometric parameters (Å, °)

Cu1—N2	1.996 (2)	Cu1—N3	1.995 (2)
Cu1—N5	1.993 (2)	Cu1—O2	2.813 (3)
Cu1—N4	2.002 (2)	Cu1—O3	2.424 (4)
N2—Cu1—N4	173.10 (9)	N4—Cu1—O2	86.60 (8)
N2—Cu1—O2	87.81 (8)	N4—Cu1—O3	96.78 (12)
N2—Cu1—O3	88.80 (12)	N3—Cu1—N2	82.67 (9)
N5—Cu1—N2	101.74 (9)	N3—Cu1—N4	92.88 (9)
N5—Cu1—N4	82.40 (9)	N3—Cu1—O2	85.74 (9)
N5—Cu1—N3	174.46 (9)	N3—Cu1—O3	93.72 (14)
N5—Cu1—O2	91.06 (9)	O3—Cu1—O2	176.61 (11)
N5—Cu1—O3	89.74 (14)		

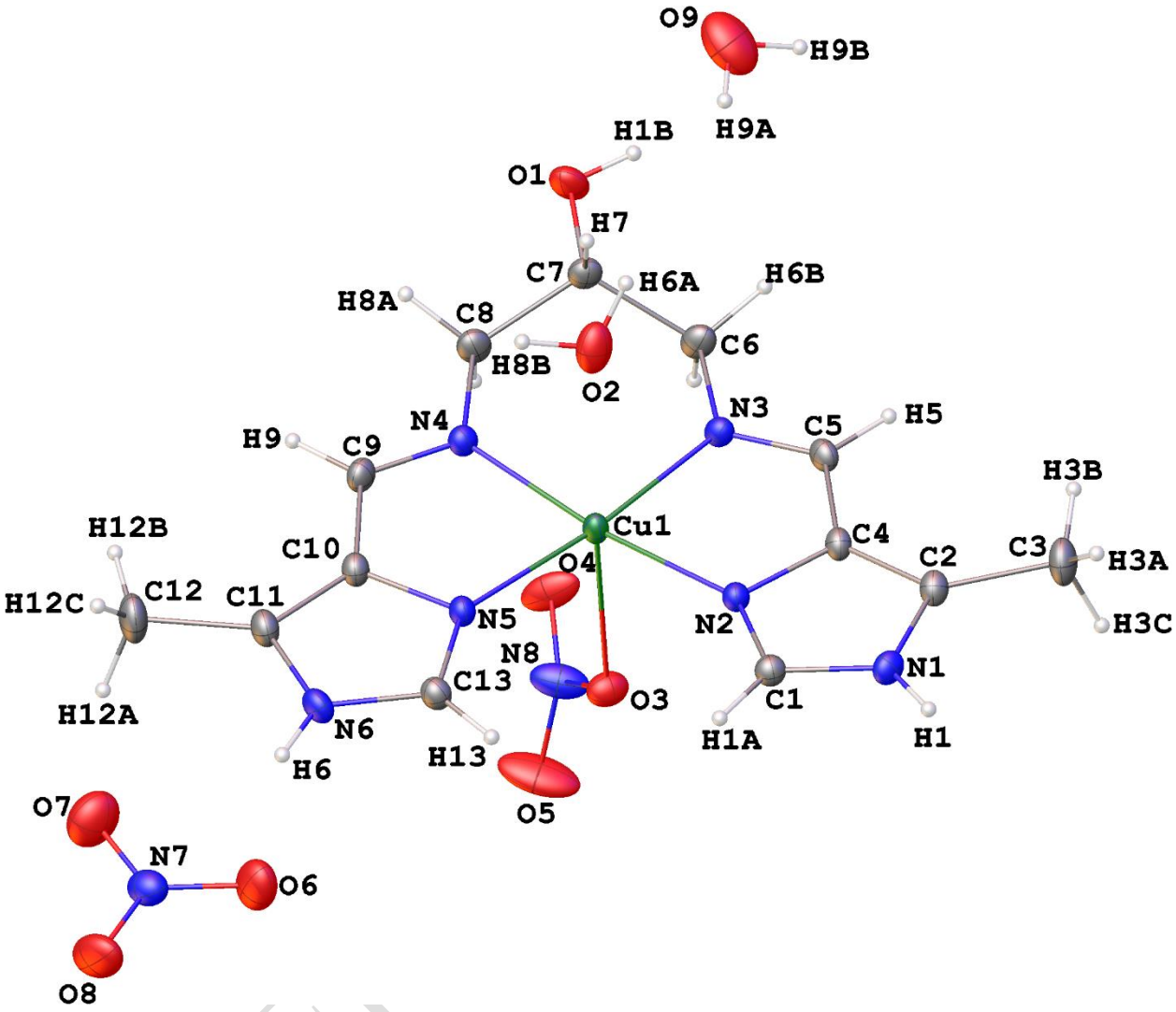

Figure 1. Crystal structure of complex 4. Displacement ellipsoids are drawn at the 30% probability level.

4. CONCLUSION

The organic ligand H_3L incorporating two pyrazole moieties showed a similar coordination mode in the complexes prepared and characterized by FTIR and UV-Vis spectroscopic methods, room temperature magnetic moment and molar conductivity measurements. The structure of the copper complex (**4**) was determined by single-crystal X-ray diffraction. The ligand acts as neutral tetradentate in all the complexes, its hydroxyl group remaining non-coordinated. In complexes **2**, **3** and **5** the metal ions are situated in N_4 inner. In all structures, the Schiff base H_3L acts as a tetradentate ligand through the nitrogen atoms of the azomethine functions and the sp^2 nitrogen atoms of the imidazole moieties. The environments of Co(II) (**2**) and Ni(II) (**3**) are described as square planar geometries. The environment of Zn(II) in the paramagnetic complex (**5**) can be described as square pyramidal of tetrahedral geometry. In the complex **1**, the Mn ion is situated in a N_4O_2 inner, and the environment is best described as octahedral geometry. The X-ray diffraction structure of complex **4** shows a slightly distorted square-based pyramidal geometry around the Cu(II).

Supplementary data

CCDC−2285926 contains the supplementary crystallographic data for the complex **4**. These data can be obtained free of charge via www.ccdc.cam.ac.uk/conts/retrieving.html, or from the Cambridge Crystallographic Data Centre, 12 Union Road, Cambridge CB2 1EZ, UK

REFERENCES

1. Shehnaz, Siddiqui WA, Raza MA, Ashraf A, Ashfaq M, Tahir MN, Niaz S. Structure elucidation single X-ray crystal diffraction studies, Hirshfeld surface analysis, DFT and antibacterial studies of sulfonamide functionalized Schiff base copper (II) and zinc (II) complexes. J. Mol. Struct. 2024;1295;136603. https://doi.org/10.1016/j.molstruc.2023.136603
2. Ghassemzadeh M, Faghani F, Shirkhani S, Mohsenzadeh F, Aghapoor K, Tahghighi A, Neumüller, B. Novel cobalt(II) complex of a new 24-membered macrocyclic bis-Schiff base bearing 3-mercapto-1,2,4-triazole: Synthesis, characterization, thermal and biological investigations. J. Mol. Struct. 2024;1295:136573. https://doi.org/10.1016/j.molstruc.2023.136573
3. Bao R-D, Song X-Q, Kong Y, Li F-F, Liao W-H, Zhou J, Zhang J-H, Zhao Q-H, Xu J-Y, Chen C-S, Xie M-J. A new Schiff base copper(II) complex induces cancer cell growth inhibition and apoptosis by multiple mechanisms. J. Inorg. Biochem. 2020;208:111103. https://doi.org/10.1016/j.jinorgbio.2020.111103
4. Liu C, Chen M-X, Li M. Synthesis, crystal structures, catalytic application and antibacterial activities of Cu(II) and Zn(II) complexes bearing salicylaldehyde-imine ligands. Inorg. Chim. Acta 2020;508:119639. https://doi.org/10.1016/j.ica.2020.119639
5. Saikumari N. Synthesis and characterization of amino acid Schiff base and its copper (II) complex and its antimicrobial studies. Mater. Today: Proc. 2021;47:1777–1781. https://doi.org/10.1016/j.matpr.2021.02.607
6. Malav R, Ray S. Recent developments on the synthesis of copper and cobalt-Schiff base complexes and their assessment as anti-tuberculosis drugs. Chem. Pap. 2024;78(8):4623–4646. https://doi.org/10.1007/s11696-024-03425-2
7. Chowdhury H, Bera R, Rizzoli C, Bieńko D, Adhikary C. Double end-on azido derivative of a tridentate (NNO) Schiff base dimeric copper(II) complex: synthesis, X-ray structure, magnetic property and catalytic effectiveness. J. Coord. Chem. 2020;73(20–22):3062–3078. https://doi.org/10.1080/00958972.2020.1836360
8. Köse A, Güngör Ö, Ballı JN, Erkan S. Synthesis, characterization, non-linear optical and DNA binding properties of a Schiff base ligand and its Cu(II) and Zn(II) complexes. J. Mol. Struct. 2022;1268:133750. https://doi.org/10.1016/j.molstruc.2022.133750
9. Shen W-Y, Jia C-P, Liao L-Y, Chen L-L, Hou C, Liu Y-H, Liang H, Chen Z-F. Copper(II) Complexes of Halogenated Quinoline Schiff Base Derivatives Enabled Cancer Therapy through Glutathione-Assisted Chemodynamic Therapy and Inhibition of Autophagy Flux. J. Med. Chem. 2022;65(6):5134–5148. https://doi.org/10.1021/acs.jmedchem.2c00133
10. Kumari P, Choudhary M, Kumar A, Yadav P, Singh B, Kataria R, Kumar V. Copper(II) Schiff base complexes: Synthetic and medicinal perspective. Inorg. Chem. Commun. 2023;158:111409. https://doi.org/10.1016/j.inoche.2023.111409
11. Dionízio TP, dos Santos AC, da Silva FP, da Silva Moura F, D'Elia E, dos Santos Garrido FM, Medeiros ME, Casellato, A. Copper(II) Schiff Base Complex with Electrocatalytic Activity Towards the Oxygen Reduction Reaction and Its Catalase Activity. Electrocatalysis 2021;12(2):137–145. https://doi.org/10.1007/s12678-020-00636-5
12. Al-Hussein MFI, Adam MSS. (2020). Catalytic evaluation of copper (II) N-salicylidene-amino acid Schiff base in the various catalytic processes. Appl. Organomet. Chem. 2020,34(6):e5598. https://doi.org/10.1002/aoc.5598

13. Jurowska A, Hodorowicz M, Arabasz M, Szklarzewicz J. Protonated amino alcohols as cations in synthesis of vanadium(V) complexes with Schiff base ligands as potential insulin-mimetic agents. J. Mol. Struct. 2024;1305:137722. https://doi.org/10.1016/j.molstruc.2024.137722
14. Shahraki S. Schiff base compounds as artificial metalloenzymes. Colloids and Surf., B 2022;218:112727. https://doi.org/10.1016/j.colsurfb.2022.112727
15. Jasińska A, Szklarzewicz J, Jurowska A, Hodorowicz M, Kazek G, Mordyl B, Głuch-Lutwin M. V(III) and V(IV) Schiff base complexes as potential insulin-mimetic compounds – Comparison, characterization and biological activity. Polyhedron 2022;215:115682. https://doi.org/10.1016/j.poly.2022.115682
16. Pesqueira NM, Morlet-Savary F, Schmitt M, Carvalho-Jr VP, Goi BE, Lalevée J. Advancing photopolymerization and 3D printing: High-Performance Ni^{II} complexes bearing N_2O_2 Schiff-base ligands as photocatalysts. Eur. Polym. J. 2024;216:113279. https://doi.org/10.1016/j.eurpolymj.2024.113279
17. Ding L, Zhang Y, Chen X, Lü X. Ni^{2+}-template mechanism to the nonsymmetrical Salen-type Schiff-base Ni^{2+} complex with effective catalysis on styrene polymerization. Inorg. Chem. Commun. 2017;76:100–102. https://doi.org/10.1016/j.inoche.2016.12.001
18. Mudi PK, Bandopadhyay N, Joshi M, Shit M, Paul S, Choudhury AR, Biswas B. Schiff base triggering synthesis of copper(II) complex and its catalytic fate towards mimics of phenoxazinone synthase activity. Inorg. Chim. Acta 2020;505:119468. https://doi.org/10.1016/j.ica.2020.119468
19. Sheldrick GM. SHELXT–Integrated space-group and crystal-structure determination. Acta Crystallogr., Sect. A: Found. Adv. 2015;71(1):3–8. https://doi.org/10.1107/S2053273314026370
20. Sheldrick GM. Crystal structure refinement with SHELXL. Acta Crystallogr., Sect. C: Struct. Chem. 2015;71(1):3–8. https://doi.org/10.1107/S2053229614024218
21. Farrugia LJ. WinGX and ORTEP for Windows: an update. J. Appl. Crystallogr. 2012;45(4):849–854. https://doi.org/10.1107/S0021889812029111
22. Kane CH, Tinguiano D, Tamboura FB, Thiam IE, Barry AH, Gaye M, Retailleau P. Synthesis and characterization of novel M(II) (M = Mn(II), Ni(II), Cu(II) or Zn(II)) complexes with tridentate N_2,O-donor ligand (*E*)-2-amino-*N*'-[1-(pyridin-2-yl)-ethylidene]benzohydrazide. Bull. Chem. Soc. Ethiop. 2016;30(1):101–110. https://doi.org/10.4314/bcse.v30i1.9
23. Sarr M, Diop M, Thiam IE, Gaye M, Barry AH, Alvarez N, Ellena J. Co-crystal structure of a dinuclear (Zn-Y) and a trinuclear (Zn-Y-Zn) complexes derived from a Schiff base ligand. Eur. J. Chem. 2018;9(2):67–73. https://doi.org/10.5155/eurjchem.9.2.67-73.1688
24. Diop A, Sarr M, Diop M, Thiam IE, Barry AH, Coles S, Orton J, Gaye, M. Metal transition complexes of tridentate Schiff base ligands derived from 2-hydrazinopyridine: synthesis, spectroscopic characterization and X-ray structures. Transition Met. Chem. 2019;44(5):415–423. https://doi.org/10.1007/s11243-019-00317-3
25. Geary, WJ. The use of conductivity measurements in organic solvents for the characterisation of coordination compounds. Coord. Chem. Rev. 1971;7(1):81–122. https://doi.org/10.1016/S0010-8545(00)80009-0
26. Khan TA, Naseem S, Azim Y, Parveen S, Shakir M. Metal-ion directed synthesis of binuclear octaazamacrocyclic complexes of manganese(II), cobalt(II), nickel(II), copper(II) and zinc(II) and their physico-chemical studies. Transition Met. Chem. 2007;32(6):706–710. https://doi.org/10.1007/s11243-007-0233-3
27. Brudenell SJ, Spiccia L, Bond AM, Fallon GD, Hockless DCR, Lazarev G, Mahon PJ, Tiekink, ERT. Structural, Spectroscopic, and Electrochemical Studies of Binuclear Manganese(II) Complexes of Bis(pentadentate) Ligands Derived from Bis(1,4,7-triazacyclononane) Macrocycles. Inorg. Chem. 2000;39(5):881–892. https://doi.org/10.1021/ic9814470

28. Nejo AA, Kolawole GA, Nejo AO. Synthesis, characterization, antibacterial, and thermal studies of unsymmetrical Schiff-base complexes of cobalt(II). J. Coord. Chem. 2010;63(24):4398–4410. https://doi.org/10.1080/00958972.2010.532871
29. Manhas BS, Verma BC, Kalia SB. Spectral and magnetic studies on normal cobalt(II) planar and cobalt(III) octahedral, spin-crossover cobalt(III) octahedral and planar-tetrahedral cobalt(II) carbodithioates. Polyhedron 1995;14(23):3549–3556. https://doi.org/10.1016/0277-5387(95)00178-U
30. Biswas A, Drew MG, Ghosh, A. Nickel(II) and copper(II) complexes of unsymmetrical tetradentate reduced Schiff base ligands. Polyhedron 2010;29(3):1029–1034. https://doi.org/10.1016/j.poly.2009.12.006
31. Sanatkar TH, Khorshidi A, Sohouli E, Janczak J. Synthesis, crystal structure, and characterization of two Cu(II) and Ni(II) complexes of a tetradentate N_2O_2 Schiff base ligand and their application in fabrication of a hydrazine electrochemical sensor. Inorg. Chim. Acta 2020;506:119537. https://doi.org/10.1016/j.ica.2020.119537
32. Emara AAA, Saleh AA, Adly OMI. Spectroscopic investigations of new binuclear transition metal complexes of Schiff bases derived from 4,6-diacetylresorcinol and 3-amino-1-propanol or 1,3-diamino-propane. Spectrochim. Acta Part A 2007;68(3):592–604. https://doi.org/10.1016/j.saa.2006.12.034
33. Abou-Hussein AA, Linert W. Synthesis, spectroscopic studies and inhibitory activity against bactria and fungi of acyclic and macrocyclic transition metal complexes containing a triamine coumarine Schiff base ligand. Spectrochim. Acta Part A. 2015;141:223–232. https://doi.org/10.1016/j.saa.2015.01.063
34. Addison AW, Rao TN, Reedijk J, van Rijn J, Verschoor GC. Synthesis, structure, and spectroscopic properties of copper(II) compounds containing nitrogen–sulphur donor ligands; the crystal and molecular structure of aqua[1,7-bis(N-methylbenzimidazol-2′-yl)-2,6-dithiaheptane]copper(II) perchlorate. J. Chem. Soc., Dalton Trans. (1984;(7):1349–1356. https://doi.org/10.1039/DT9840001349
35. Reinen D, Atanasov M. Symmetry and vibronic coupling: The stereochemistry and the ground state potential surface of Cu^{2+} in five-coordination. Chem. Phys. 1991;155(2):157–171. https://doi.org/10.1016/0301-0104(91)87016-O
36. Bhaumik PK, Jana S, Chattopadhyay S. Synthesis and characterization of square planar and square pyramidal copper(II) compounds with tridentate Schiff bases: Formation of a molecular zipper via H-bonding interaction. Inorg. Chim. Acta 2012; 390:167–177. https://doi.org/10.1016/j.ica.2012.04.004